

Soft Matter

Accepted Manuscript



This is an *Accepted Manuscript*, which has been through the Royal Society of Chemistry peer review process and has been accepted for publication.

Accepted Manuscripts are published online shortly after acceptance, before technical editing, formatting and proof reading. Using this free service, authors can make their results available to the community, in citable form, before we publish the edited article. We will replace this *Accepted Manuscript* with the edited and formatted *Advance Article* as soon as it is available.

You can find more information about *Accepted Manuscripts* in the [Information for Authors](#).

Please note that technical editing may introduce minor changes to the text and/or graphics, which may alter content. The journal's standard [Terms & Conditions](#) and the [Ethical guidelines](#) still apply. In no event shall the Royal Society of Chemistry be held responsible for any errors or omissions in this *Accepted Manuscript* or any consequences arising from the use of any information it contains.

Submitted to Soft Matter

Revised 5th June

Paper

Experimental Verification of Fracture Mechanism for Polymer Gels with controlled network structure

Takamasa Sakai*, Yuki Akagi, Shinji Kondo and Ungil Chung

Department of Bioengineering, Graduate School of Engineering, The University of Tokyo, 7-3-1 Hongo, Bunkyo-ku, Tokyo 113-8656, Japan

** To whom correspondence should be addressed.*

Abstract

Recently, polymer gels draw much attention as scaffolds for regenerative medicine, soft actuator, and functional membrane. These applications need tough and robust polymer gels as represented by the double network gels. To fully understand this mechanism and develop further advanced polymer gels, we need to fully understand the molecular origin of fracture energy for conventional polymer gels, which is inhibited by the inherent heterogeneity. In this paper, we show the experimental results on the fracture of model polymer gels with controlled network structure, and discuss the mechanism of the fracture of polymer gels.

I. Introduction

Elastomers are important material for a variety of applications including tires, shock absorbing materials, soft actuators, and biomaterials. To tailor the physical properties for each application, the molecular understanding of physical properties is of peculiar importance. However, at this point, we do not have definite pictures for the molecular origin of physical properties. For example, the elastic modulus (G) is explained by the relationship with the number density of elastically effective chains.^{1,2} We have two popular models for the elastic modulus including the affine network¹ and phantom network³ models, of which validity or applicability is not clarified. This problem is caused by the difficulty in the control of the network structures and in the direct observation of the network structure. Because the elastomers have complicated and heterogeneous structure⁴ including heterogeneous distribution of crosslinking, chain entanglements, dangling ends, and loops, we cannot estimate the structural parameters of elastomers from the feed condition. In addition, we cannot observe these complicated substructures with direct visualization by TEM and SEM. To understand the molecular origin of physical properties, as a first step, we need to perform a series of studies on elastomers with controlled network structure.

Recently, we succeeded in fabricating homogeneous polymer network system from a novel molecular design in prepolymer architecture and reaction system.^{5,6} We synthesized two kinds of tetra-armed prepolymers with mutually reactive end groups, which are amine and activated ester. We can fabricate polymer gels by mixing two aqueous solutions of the prepolymers at around the physiological condition. The unique tetra-armed prepolymers completely inhibit the self-biting reaction, and form the elastically effective chains efficiently. The ionic equilibrium of amine species allows

us to control the reaction rate and to mix two prepolymer solutions, resulting in homogeneous network structure.⁷ We named this polymer network swollen in aqueous solution as Tetra-PEG gel, and validated the homogeneity by means of the small angle neutron scattering^{8,9} and nuclear magnetic resonance¹⁰. These measurements clarified that the heterogeneity of Tetra-PEG gel was strongly suppressed over the other structure-controlled polymer networks including “model networks”. Using Tetra-PEG gel as a model system, we, for the first time, observed the crossover of elastic modulus from the phantom to the affine network models with an increase in the polymer volume fraction,¹¹ which was originally predicted by Flory in 1977.¹² These experimental results strongly suggested that Tetra-PEG gel is a promising model system contributing to the molecular understanding on the physical properties of elastomeric materials.

In this paper, we focus on the fracture of polymer gels. In general, the most important parameter related to the fracture is the fracture energy (T_0), which is the energy required to propagate a unit length of crack. The Lake-Thomas theory describes T_0 as the energy needed to break the chemical bonds per unit cross-section on the fracture surface as,¹³

$$T_0 = \left(\frac{3}{8}\right)^{1/2} \nu LNU \quad (1)$$

, where ν is the number of elastically effective chain per unit volume, L is the displacement length, N is the degree of polymerization of network strand, and U is the total bond energy of monomeric unit. Originally, the value of L is related to the strand length of the network as $L \approx R_0 \approx aN^{1/2}$ (a : monomer length); however, there is an ambiguity in L , because there is no quantitative validation of the Lake-Thomas model. Although the quantitative validation has been inhibited by the heterogeneity, the

qualitative validation has been done by Gent et al.^{14, 15} They observed the relationship between T_0 and G as, $T_0 \sim G^{-1/2}$, which is given from eqn 1, when we assume that $\nu \sim G$ and $N \sim G^{-1}$. However, in general, when we use R_0 in eqn 1, we need to add the enhancement factor (k) as^{14, 16, 17}

$$T_0 = \left(\frac{3}{8}\right)^{1/2} k \nu R_0 N U \quad (2)$$

The value of k strongly depends on the system, and in the range from unity to thousands. Notably, the popular double network gels with extremely high fracture toughness have high k up to thousands.¹⁸⁻²⁰ Because the effect of k is so strong, the molecular origin of k is of great importance for designing the advanced materials.

To investigate the fracture energy, we prepared Tetra-PEG gels with tuned degree of strand polymerization between crosslinks (N_c), polymer volume fraction (ϕ_0), connectivity (p), and heterogeneous distribution in strand length. Through the analysis of Tetra-PEG gels, we discuss the effects of structural parameters on fracture energy based on the Lake-Thomas model and finally discuss the enhancement factor.

II. Experimental procedure

A. Synthesis and characterization of prepolymers

Tetra-PEG gel consists of two kinds of prepolymers; Tetra poly(ethylene glycol)-succinimidyl carbonate (TetraPEG-OSu) and Tetra poly(ethylene glycol)-amine (TetraPEG-NH₂). These prepolymers were synthesized from Tetra poly(ethylene glycol) (TetraPEG-OH). Each prepolymer was characterized by ¹H NMR (JEOL JNM-AL 300MHz) and gel permeation chromatography (TOSOH HLC-8220) system.^{11, 22-23}

B. Fabrication of Tetra-PEG gels

We fabricated four kinds of Tetra-PEG gels: (i) conventional Tetra-PEG gel, (ii) p -tuned Tetra-PEG gel, (iii) hetero Tetra-PEG gel, and (iv) bimodal Tetra-PEG gel.

Equimolar quantities of TetraPEG-NH₂ and TetraPEG-OSu (ϕ_{\square} : 0.034-0.12) were dissolved in phosphate buffer (pH7.4) and phosphate-citric acid buffer (pH5.8), respectively. The ionic strength of buffer solution was varied to maintain the solution pH. In order to tune the reaction conversion (p), the TetraPEG-OSu solution was incubated at 25 °C for a series of times (t_{deg}). After the incubation time, TetraPEG-NH₂ and TetraPEG-OSu solutions were mixed, and the resulting solution was poured into the mold. At least 12 hours were allowed for the completion of the reaction before the following experiment was performed. The detailed experimental conditions are listed in Table 1-3.

Table 1. Experimental conditions for the conventional Tetra-PEG gels and p -tuned Tetra-PEG gels.

Combination of TetraPEG's (g/mol)	ϕ_{\square}	Ionic strength of Buffers (mM)	Incubation time of TetraPEG-OSu (min)
5k-5k	0.034	50	0
	0.050		
	0.066		
	0.081	100	
	0.12		
10k-10k	0.034	25	0
	0.050		
	0.066		
	0.081	50	
	0.12		
20k-20k	0.034	50	0
	0.050		
	0.066		

	0.081	100	
	0.12		
40k-40k	0.034	25	0
	0.050		
	0.066		
	0.081	50	
	0.12		
20k-20k	0.081	100	20
			80
			120
			160
			200
			240
			320
			400

Table 2. Experimental conditions for the hetero Tetra-PEG gels.

Combination of TetraPEG's (g/mol)	ϕ_{\square}	Ionic strength of Buffers (mM)
5k-10k	0.034	50
	0.050	
	0.066	
	0.081	100
	0.12	
5k-20k	0.034	25
	0.050	50
	0.066	
	0.081	
	0.12	100
10k-20k	0.034	25
	0.050	
	0.066	
	0.081	50
	0.12	

Table 3. Experimental conditions for the bimodal Tetra-PEG gels.

Combination of TetraPEG's (g/mol)	20 kg/mol Tetra-PEG mol	ϕ_{\square}	Ionic strength of Buffers
-----------------------------------	-------------------------	------------------	---------------------------

TetraPEG-NH ₂ [mM]		TetraPEG-OSu [mM]		fraction (<i>r</i>)		(mM)
5k	20k	5k	20k			
4.0	0	4.0	0	0	0.034	25
4.0	0	3.0	1.0	0.125	0.046	
4.0	0	2.0	2.0	0.25	0.058	
4.0	0	1.0	3.0	0.375	0.070	
4.0	0	0	4.0	0.5	0.081	50
3.0	1.0	0	4.0	0.675	0.092	
2.0	2.0	0	4.0	0.75	0.103	100
1.0	3.0	0	4.0	0.875	0.113	
0	4.0	0	4.0	1	0.124	

C. Infrared (IR) measurement

The gel samples were prepared as cylinder shape (diameter: 15 mm, height: 7.5 mm), and immersed H₂O for 2 days in order to remove the sol fraction.

After dried in air, the samples were cut into thin films (thickness: 40 μm) using a microtome (SM2000R, Leica). These dried samples were swollen in D₂O, and then soaked in a mixture solvent of D₂O and oligo-PEG ($M_w = 0.40$ kg/mol) (v/v=1/1). The IR measurements for these samples were performed using a JASCO FT-IR-6300 equipped with a deuterated triglycine sulfate (DTGS) detector, where 128 scan were coadded at a resolution of 4 cm⁻¹ for samples.

D. Tearing test

The tearing test was performed in air using a stretching machine (Tensilon RTC-1150A, Orientec Co.). The samples were cut into the shape, which has standardized JIS-K 6252 as 1/2 sizes (50 mm x 7.5 mm x 1 mm, the length of initial notch is 20 mm) using a gel cutting machine (Dumb Bell Co., Ltd.). The two arms of the test sample were clamped and one arm was pulled upward at a constant velocity (40 and 500 mm/min), while the other arm was maintained stationary. The tearing force F was recorded.

III. Results and Discussion

A. Fabrication of Tetra-PEG gels

We fabricated four kinds of Tetra-PEG gels: (i) conventional Tetra-PEG gel, (ii) *p*-tuned Tetra-PEG gel, (iii) hetero Tetra-PEG gel, and (iv) bimodal Tetra-PEG gel.

- (i) Conventional Tetra-PEG gel (Fig.1 (a))²¹: Equimolar amounts of TetraPEG-NH₂ and TetraPEG-OSu with the same molecular weight were used as prepolymers. The molecular weight of prepolymers (M_w) were tuned in 5, 10, 20 and 40 kg/mol and resultant gels were named as named 5k, 10k, 20k and 40k Tetra-PEG gel, respectively. The polymer volume fraction (ϕ_0) was tuned from 0.034 to 0.12.
- (ii) *p*-tuned Tetra-PEG gel (Fig.1 (b))²¹: *p*-tuned Tetra-PEG gels is fabricated by using partially hydrolyzed TetraPEG-OSu as a prepolymer. Prior to the reaction, Tetra-PEG-OSu was dissolved in the aqueous buffer solution and allowed to hydrolyze for a certain period of time ($t_{deg} = 0, 20, 80, 120, 160, 200, 240, 320$ and 400 min). The values of M_w and ϕ_0 were fixed to 20 kg/mol and 0.081, respectively.
- (iii) Hetero Tetra-PEG gel (Fig.1 (c))²²: Equimolar amounts of TetraPEG-NH₂ and TetraPEG-OSu with different molecular weights were used as prepolymers. The polymer gels formed from the combinations of prepolymers with 5k-10k, 5k-20k and 10k-20k were named as 5k-10k, 5k-20k and 10k-20k Tetra-PEG hetero gel, respectively. The value of ϕ_0 was tuned from 0.034 to 0.12.
- (iv) Bimodal Tetra-PEG gel (Fig.1 (d))²³: We mixed 5k and 20k Tetra-PEG prepolymers with the molar ratio being tuned ($r = (20k \text{ Tetra-PEG prepolymer})/(\text{total prepolymer})$), while maintaining the equimolar condition of

amine and activated ester. The molar concentration of prepolymers was fixed to 8.0×10^{-3} mol/L. We started from the mixing of 5k Tetra-PEG-NH₂ and 5k Tetra-PEG-OSu, which forms Tetra-PEG unimodal gel with molecular weight of network strand of 2.5k g/mol ($r = 0$), then we gradually exchanged 5k Tetra-PEG-OSu to 20k Tetra-PEG-OSu. It should be noted that Tetra-PEG gel formed from 5k Tetra-PEG-NH₂ and 20k Tetra-PEG-OSu ($r = 0.5$) corresponds to Tetra-PEG unimodal gel with molecular weight of network strand of 6.25k g/mol. Then, we gradually exchanged 5k Tetra-PEG-NH₂ to 20k Tetra-PEG-NH₂, finally resulting in Tetra-PEG unimodal gel with molecular weight of network strand of 10k g/mol ($r = 1.0$).

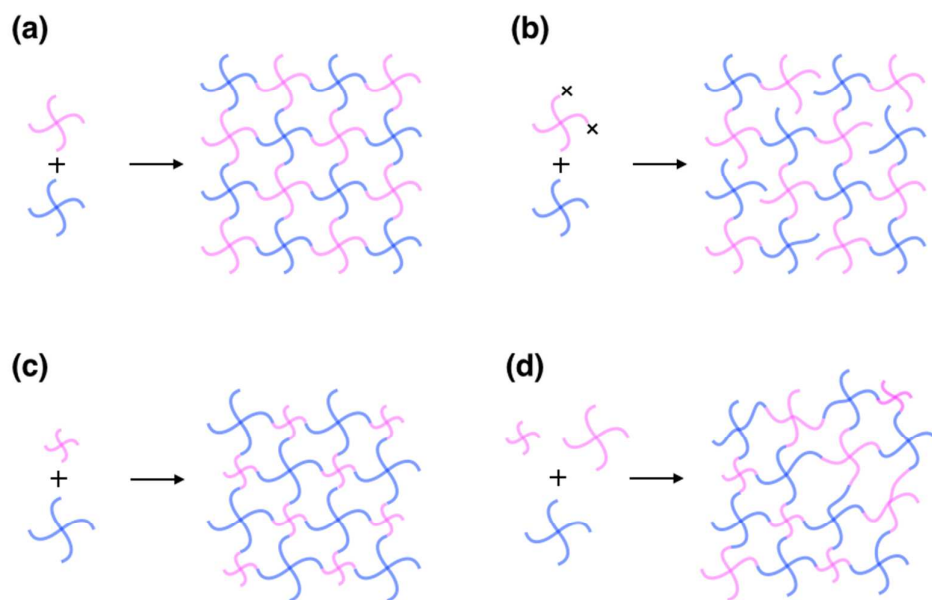


Figure 1. Schematic pictures of (a) conventional, (b) *p*-tuned, (c) hetero and (d) bimodal Tetra-PEG gels.

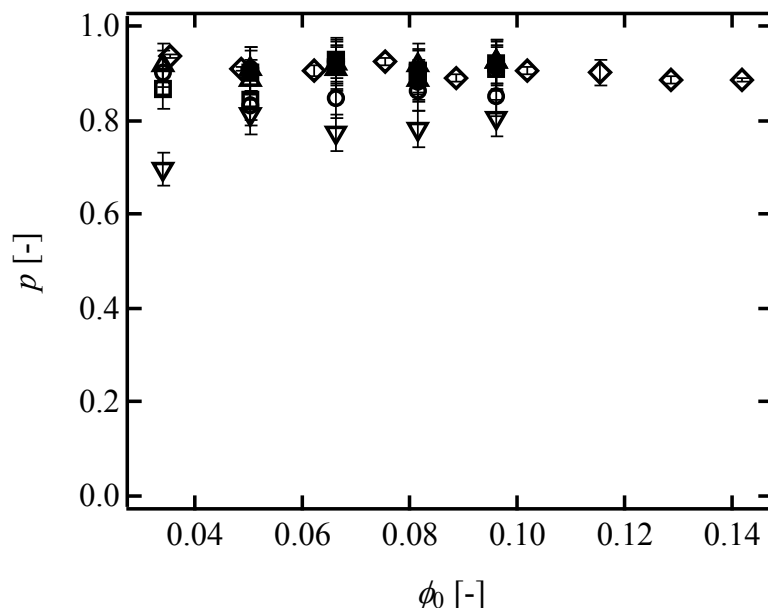


Figure 2. p as a function of ϕ_0 in conventional Tetra-PEG gel (open circles; 5k, open squares; 10k, open triangles; 20k, open lower triangles; 40k-Tetra-PEG gel), hetero Tetra-PEG gel (filled circles; 5k-10k, filled squares; 5k-20k, filled triangles; 10k-20k) and bimodal Tetra-PEG gel (rhombus; 5k-20k).

The reaction conversion (p) was estimated by FT-IR measurement for gel samples¹¹. p was estimated from the peak intensity of ionized carbonyl group (1555 cm^{-1}) and that of amide bond (1624 cm^{-1}) as follows,

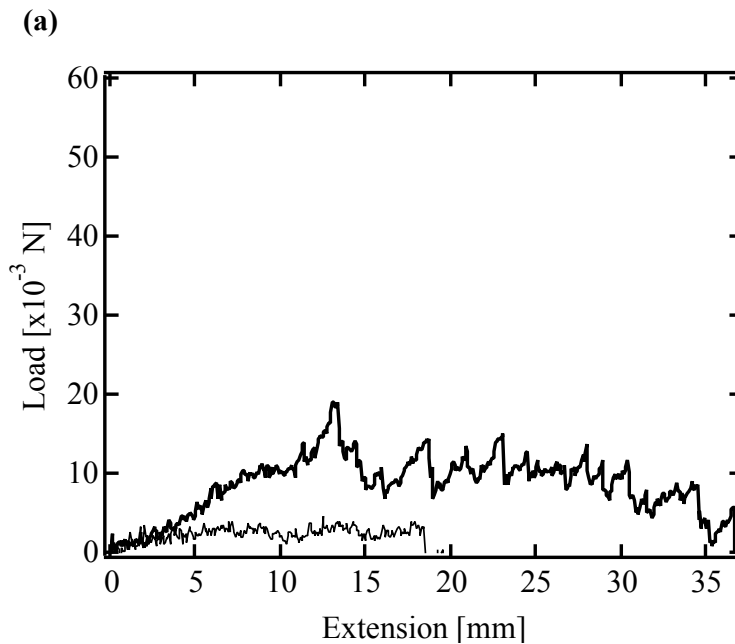
$$p = \frac{I_{amide}}{I_{amide} + I_{calboxyl}} \quad (3)$$

where I_{amide} and $I_{calboxyl}$ are the peak intensity of ionized carbonyl group and that of amide bond, respectively. The ratio of the molar absorbance coefficient of ionized carbonyl group to amide bond was estimated to be 1.0 : 1.0. The values of p were almost constant against ϕ_0 in all Tetra-PEG gels, and were 0.82 – 0.95 for 5k, 10k and

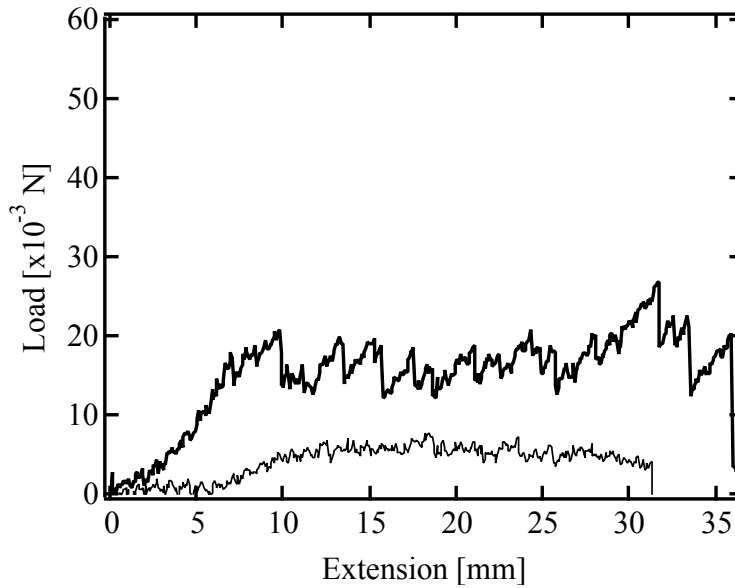
20k Tetra-PEG gels, 5k-10k, 5k-20k and 10k-20k Tetra-PEG hetero gels and Tetra-PEG bimodal gels, and p was 0.71-0.81 for 40k Tetra-PEG gel (Figure 2).

B. Estimation of fracture energy

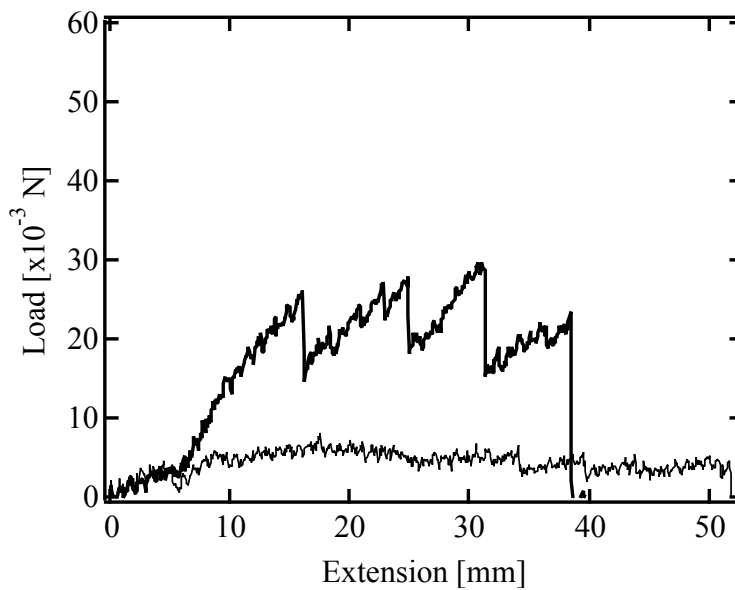
To investigate the fracture energy (T_0), we performed the tearing measurement for trouser-shaped specimens¹¹. The gel specimens were used in as-prepared state, not in equilibrium-swollen state. The one of trousers was pulled upward at a constant velocity of 40 mm/min, while the other arm was maintained stationary, and the load (F) was recorded. We performed the tearing measurements at a different velocity of 500 mm/min, and confirmed the rate-independent tearing behavior in this experimental condition. The similar rate-independent tearing behavior was observed for other gel systems.



(b)



(c)



(d)

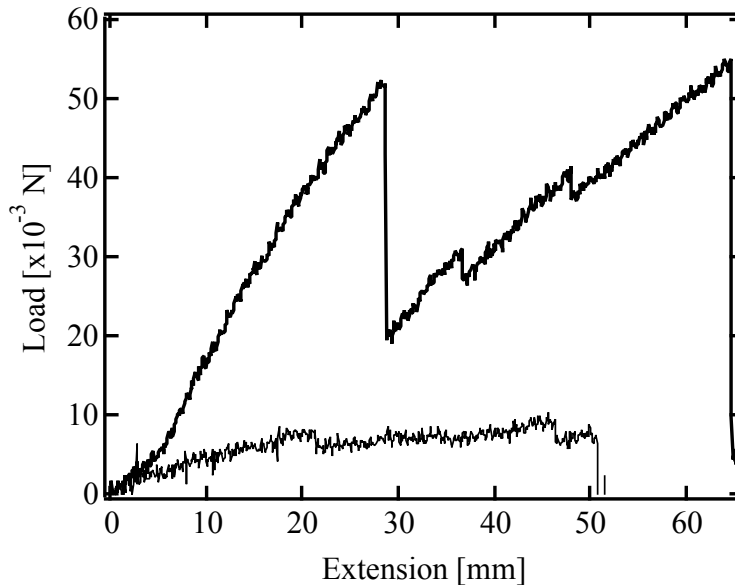


Figure 3. Tearing force-extension relationships in (a) 5k, (b) 10k, (c) 20k, (d) 40k Tetra-PEG gel (fine line, $\phi_0 = 0.034$; bold line, $\phi_0 = 0.1$).

Figure 3 shows the tearing behavior of conventional Tetra-PEG gels. In the beginning, the load value monotonously increased with an extension, where crack did not propagate. After starting the crack propagation, the load fluctuated with an extension. In the whole region of 5k and 10k, and the low ϕ_0 region of 20k and 40k Tetra-PEG gel, the steady tearing, where the degree of fluctuation is relatively small, was observed. On the other hand, the stick-slip tearing, where the degree of fluctuation is large and clear peaks were observed, was observed for 20k and 40k Tetra-PEG gel with the higher ϕ_0 region, and the tendency became prominent with increases in M_w and ϕ_0 .

We estimated different values of T_0 from the average of local maximum, the simple average and the average of local minimum values of F as,

$$T_0 = \frac{2F}{h} \quad (4)$$

, where h is the thickness of the gel samples. It should be noted that only the values of

F after starting the crack propagation were accumulated. The values of T_0 computed from the local maximum and average values of F were strongly influenced by the magnitude of stick-slip behavior, while T_0 computed from the local minimum values was little affected by the magnitude of stick-slip behavior and systematically changed against the feed conditions. Although we realize the importance of the understanding of the stick-slip behavior, in this study, we focus on T_0 computed from the minimum values of F , which indicates the minimum energy required to propagate a crack.

C. p -tuned Tetra-PEG gels

Prior to the investigation on conventional Tetra-PEG gels, we focus on the p -tuned Tetra-PEG gels.²¹ It is because the connectivity defects of the network can influence the structural parameters including ν and N . When we accept the above-mentioned scaling relationships $G \sim \nu$ and $G \sim N^{-1}$, the decrease in p will decrease ν , leading to an increase in N . If the value of N was influenced by p , we could not use the values of N directly calculated from the molecular weight of prepolymers as

$$N = M_w / 2m_{\text{PEG}} \quad (5)$$

, where m_{PEG} is the molecular weight of PEG per monomeric unit. In addition, the p -tuned Tetra-PEG gels allow us to investigate the pure effect of p on T_0 , while maintaining ϕ_0 and M_w unchanged.

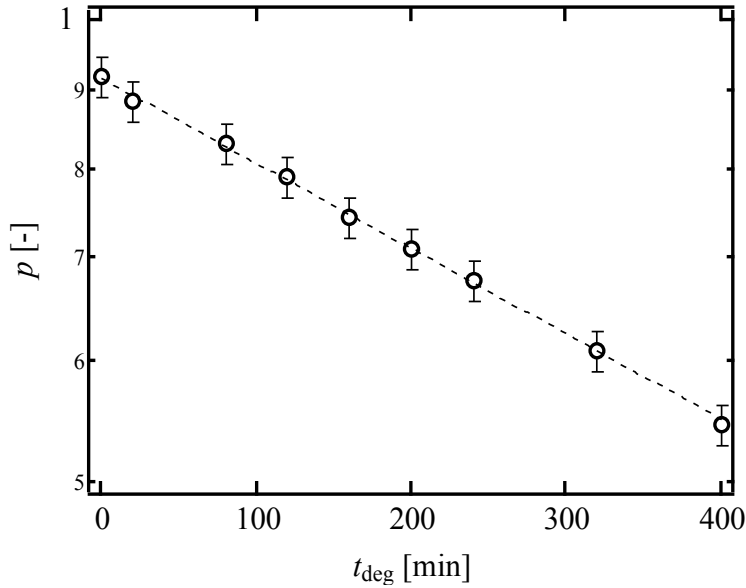


Figure 4. p as a function of t_{deg} . The dashed line is the guide line showing the relationship, $p \sim \exp(-t_{\text{deg}})$. (Reproduced from Akagi *et al.*²¹ with permission from the American Institute of Physics)

By hydrolyzing the activated ester prior to the reaction, the values of p were successfully tuned from 0.55 to 0.92 (Figure 4). The effect of p on ν can be directly predicted according to the tree-like approximation as,^{24, 25}

$$\nu = \frac{\rho\phi_0}{M_w} \left\{ \frac{3}{2} \binom{4}{3} (1-P_\infty)^3 \cdot P_\infty + \frac{4}{2} \binom{4}{4} (1-P_\infty)^4 \right\} \quad (6)$$

$$P_\infty = p \cdot P_\infty^3 + (1-p) \quad (7)$$

, where ρ ($= 1.129 \text{ g/cm}^3$) is the density of PEG, P_∞ is the probability that an arm does not lead to an infinite network, and $\binom{x}{y}$ is the usual notation for the number of combinations of x items taken y at a time: $x!/y!(x-y)!$. Notably, in the previous reports,

we have checked the validity of ν calculated by the tree-like approximation through the experimental study on elastic modulus of the p -tuned Tetra-PEG gels.²⁶

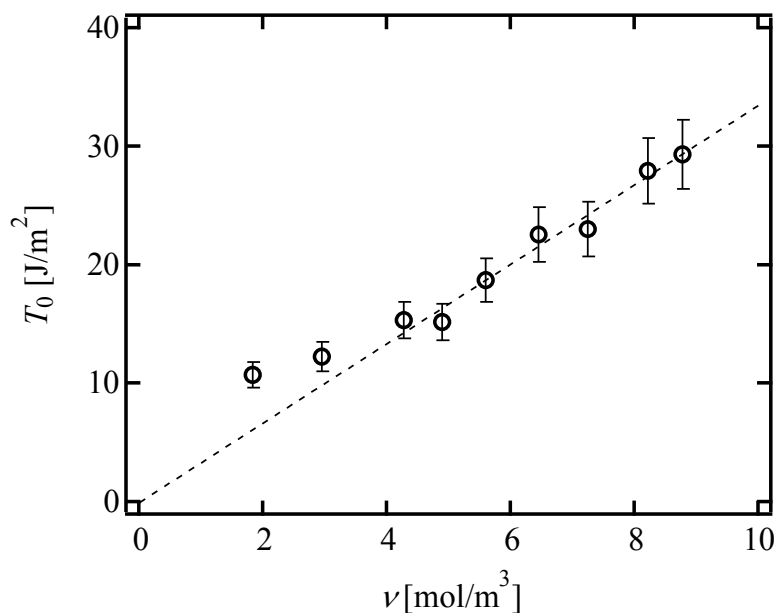


Figure 5. T_0 as a function of ν in p -tuned Tetra-PEG gel. (Reproduced from Akagi *et al.*²¹ with permission from the American Institute of Physics)

Figure 5 shows the values of T_0 against ν . As mentioned above, the change in ν was purely originated from the change in p . The dashed line represents the scaling prediction of the Lake-Thomas model, $T_0 \sim \nu$. As clearly shown in Figure 5, the experimental data obeyed the Lake-Thomas prediction in the region $\nu > 4.0$ ($p > 0.65$). This agreement in this region indicates that ν calculated by the tree-like approximation is applicable to the Lake-Thomas model, and that the term LNU does not depend on p . In the region $p > 0.65$, we can use the values of N and U calculated from eqns 5 and 8, respectively.

$$U = 357 \text{ (C-C bond)} + 2 \times 329 \text{ (C-O bond)} = 1.0 \times 10^6 \text{ J/mol} \quad (8)$$

On the other hand, in the region of $\nu < 4.0$, T_0 deviated upward from the guideline. This region well corresponds to the region where the elastic modulus cannot be predicted by ν calculated under the tree-like approximation. A massive amount of dangling chains may inhibit the mean-field-like treatment in this region. In the following analyses, we use the N and U calculated from eqns 5 and 8, because all the values of p shown in Figure 2 is higher than 0.65.

D. Conventional Tetra-PEG gels and hetero Tetra-PEG gels

In order to investigate the effects of N and ϕ_0 on T_0 , we evaluated T_0 of the conventional Tetra-PEG gels with different N and ϕ_0 .²¹ Figure 6 (open symbols) shows the values of T_0 as a function of ν ; the values of T_0 of the same N was on the same line proportional to ν . Because the difference in ν for Tetra-PEG gels with each N was purely originated from ϕ_0 , these data indicate that the slope (LNU) is independent of ϕ_0 , but dependent of N . From the linear fit, the slopes are estimated to be 0.45, 1.28, 3.15 and 9.18 for 5k, 10k, 20k and 40k Tetra-PEG gels, respectively. Here, we show the data of hetero Tetra-PEG gels (Figure 1 (c)).²² Notably, each hetero Tetra-PEG gel has a monomodal network strand length defined by the molecular weights of prepolymers (M_1 and M_2) as $N = (M_1 + M_2) / 4m_{\text{PEG}}$ (e.g. for 5k-10k Tetra-PEG hetero gel, $N = (5000 + 10000) / 4 / 44 = 85.2$). As shown in Figure 6 (filled symbols), we can observe the linear relationships for hetero Tetra-PEG gels, and the slopes increased with an increase in N ; the slopes were 0.88, 1.68 and 2.17 for 5k-10k, 5k-20k and 10k-20k hetero Tetra-PEG gels, respectively. Using the constant values of N and U calculated from eqns 5 and 8, we estimated the values of L from the slopes according to eqn 1.

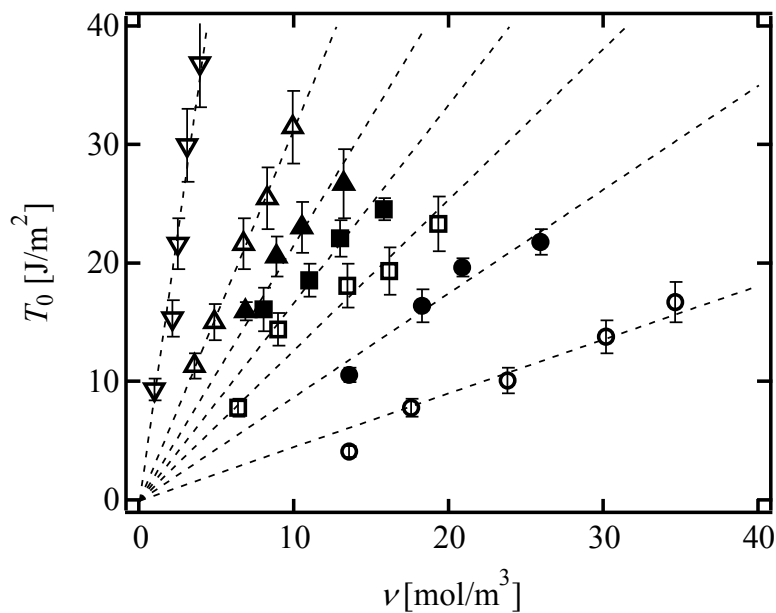


Figure 6. T_0 as a function of ν in conventional Tetra-PEG gel (open circles; 5k, open squares; 10k, open triangles; 20k, open lower triangles; 40k-Tetra-PEG gel) and hetero Tetra-PEG gel (filled circles; 5k-10k, filled squares; 5k-20k, filled triangles; 10k-20k). Linear fitting of the data are shown as the dotted lines.

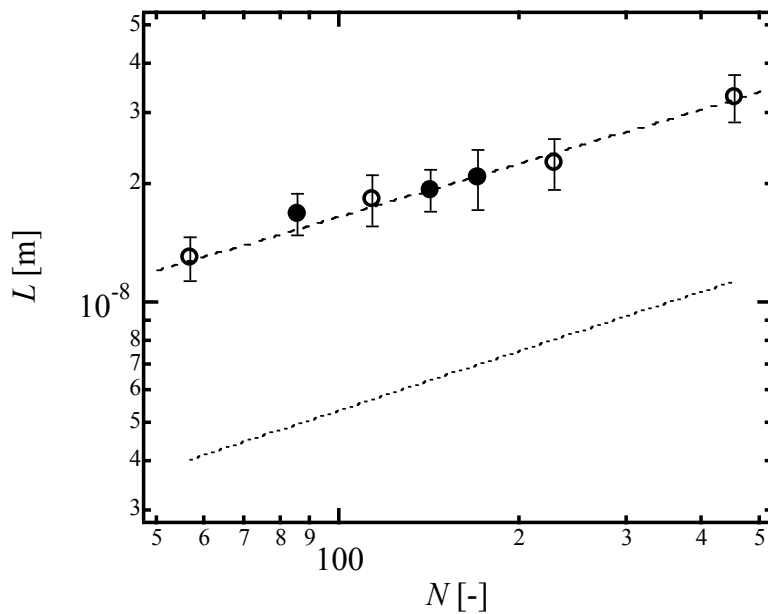


Figure 7. L as a function of N in Tetra-PEG gel (open circles) and hetero Tetra-PEG gel (filled circles).

Figure 7 shows L of conventional Tetra-PEG gels (open circles) and Tetra-PEG hetero gels (filled circles) against N . L increased from 13 to 34 nm with an increase in N . In the original Lake-Thomas model, L corresponds to R_0 ($\approx aN^{1/2}$) of virtual network chains with polymerization degree of N (dotted line in Figure 7). R_0 are calculated as $b_k N_k^{1/2}$, where b_k (0.65 nm) and N_k are the length and number of Kuhn segments, respectively.²⁷⁻²⁹ The values of N_k is derived as $N_k = 0.68N$, where we assume that the bond angles are 109.5° , and bond length of C-C and C-O are 0.154 and 0.145 nm, respectively. The values of L and R_0 have similar magnitude and N -dependence, which corresponds to, but are different from each other. According to eqn 2, we estimated k for each N and plotted it against N (Figure 8). The values of k were almost constant and approximately 3 in the range examined. These data indicate that network strands within $3R_0$ from the crack tip are extended at the fracture, and the length is determined only by N , regardless of p and ϕ_0 .

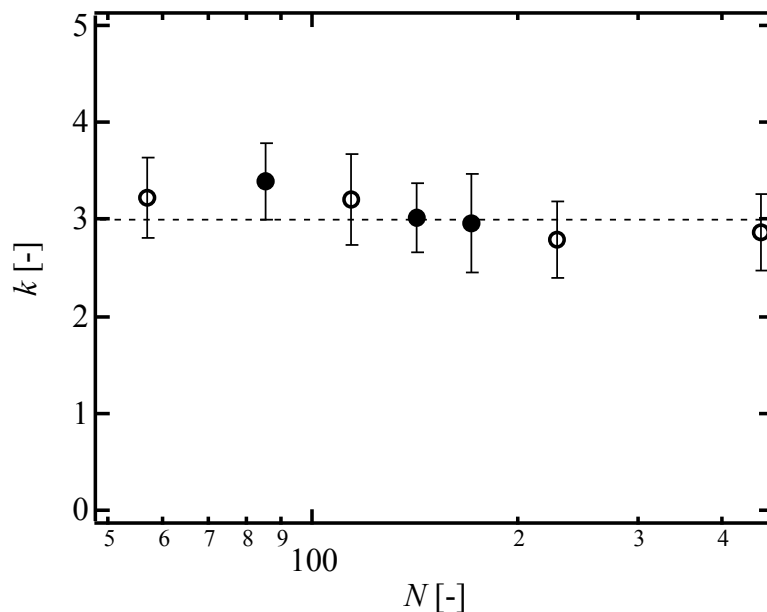


Figure 8. k as a function of N in Tetra-PEG gel (open circles) and hetero

Tetra-PEG gel (filled circles).

E. Bimodal Tetra-PEG gels

Finally, we investigated effect of another heterogeneity, i.e., heterogeneous distribution in strand length.²³ This heterogeneity was introduced by mixing three kinds of 5k and 20k Tetra-PEG prepolymers with the molar ratio being tuned (Figure 1(d), $r = (20\text{k Tetra-PEG prepolymer})/(\text{total prepolymer})$). We tuned r with fixing the molar concentration of prepolymers to 8.0×10^{-3} mol/L (Figure 1 (d)). The molecular weight of shorter strands is 2.5 kg/mol, and that of longer strands is 10 kg/mol. Although the difference in the molecular weight is not so large, we can assess the effect of heterogeneous distribution in strand length on T_0 . Figure 9 shows the T_0 of the bimodal Tetra-PEG gels. As shown in Figure 9, T_0 increased with r . Reflecting the constant p , the values of ν calculated were almost constant with a change in r . Considering the constant ν against r , the increase in T_0 is originated from other parameters including N and L . Here, we assume that the value of N in the bimodal Tetra-PEG gels is represented by the number-average degree of polymerization of prepolymers ($N_{\text{ave}} = (5000(1-r)+20000r)/2m_{\text{PEG}}$). Figure 10 shows the N_{ave} -dependence of L and guide of R_0 calculated from N_{ave} (dotted line). The values of L and R_0 have similar N_{ave} -dependence, but are different from each other. We also estimated k using eqn 2, and plotted against N in Figure 11. Although the values of k were slightly smaller than those for conventional and hetero Tetra-PEG gels, the values were similar with each other. These data indicate that the heterogeneous distribution in strand length does not significantly influence T_0 in the range of this study.

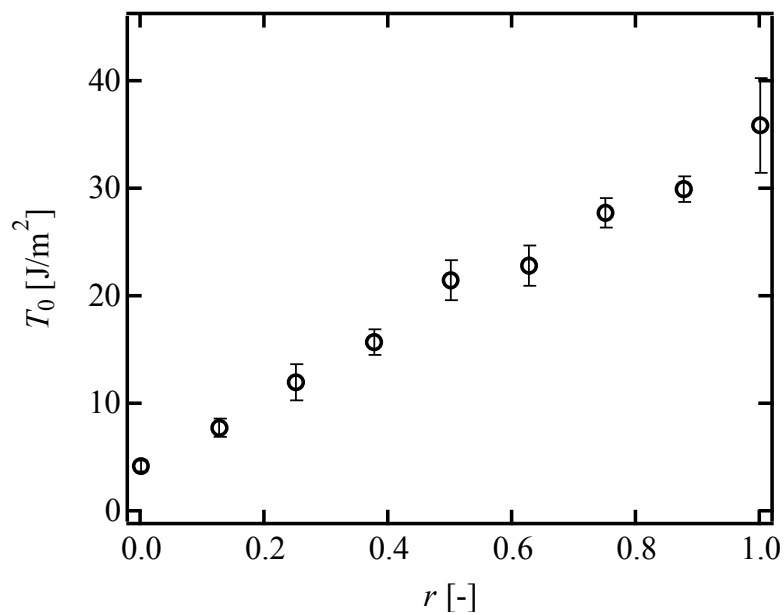


Figure 9. T_0 as a function of r in bimodal Tetra-PEG gel.

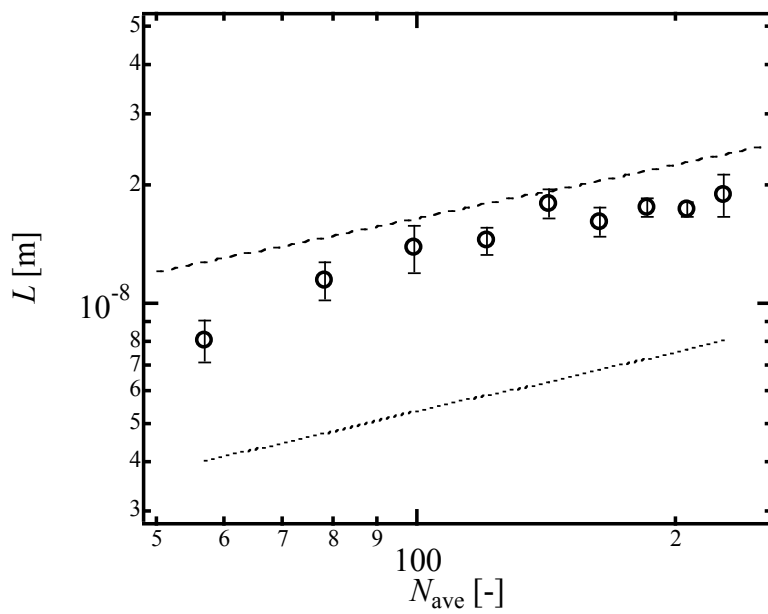


Figure 10. L as a function of N_{ave} in bimodal Tetra-PEG gel.

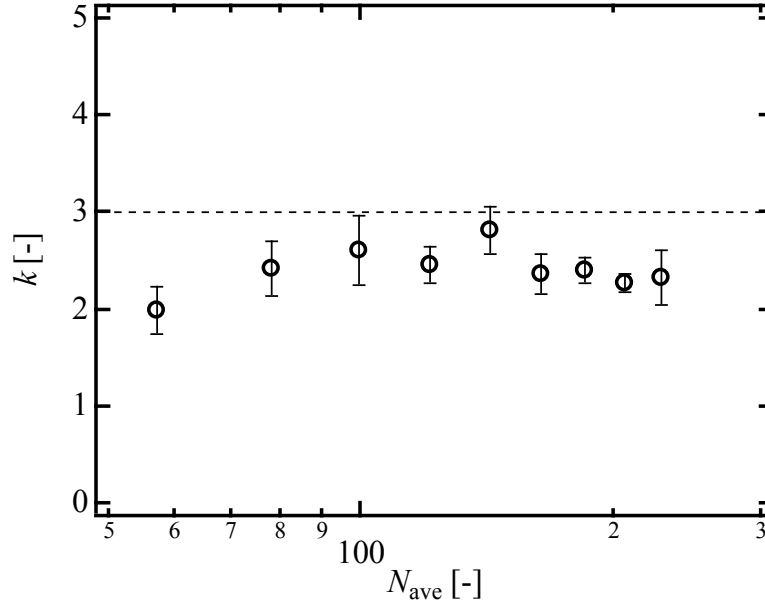


Figure 11. k as a function of N_{ave} in bimodal Tetra-PEG gel.

IV. Conclusions

In this paper, we discussed the fracture energy of polymer gels with controlled network structure. The fracture energies of Tetra-PEG gels with tuned structural parameters are fully explained by the Lake-Thomas model with $k = 3$. The value of k is universal in the range of this study; not only changes in ϕ_0 and N but also the connective heterogeneity and heterogeneous distribution in strand length did not affect the value of k . These data suggest that the enhancement factor estimated in this study can be applicable to the conventional polymer gels with the similar concentration range regardless of the degree of heterogeneity, although there is a possibility that the macroscopic heterogeneity ($\sim \mu\text{m}$), which was not observed in Tetra-PEG gel system, affects the fracture toughness. In other words, the network homogeneity does not strongly contribute to the enhancement of fracture toughness. The constant k also

suggests that it is difficult for conventional polymer gels to achieve the enhanced fracture toughness. As proposed by Gong, chain entanglements may play an important role for enhanced k .^{19, 20, 30-32}

Here, we must point out the limitation of this study; we investigated T_0 computed from the minimum values of F in the tearing measurements. We ignored the effect of tearing behavior: steady state or stick-slip. Because fracture starts at the maximum values of F , the molecular understanding of T_0 calculated from the maximum value of F is also important. To fully understand the fracture behavior, we need further investigation on the tearing behavior.

Acknowledgement

This work was supported by the Japan Society for the Promotion of Science (JSPS) through the Grants-in-Aid for Scientific Research, the Center for Medical System Innovation (CMSI), the Graduate Program for Leaders in Life Innovation (GPLLI), the International Core Research Center for Nanobio, Core-to-Core Program, A. Advanced Research Networks, and the Funding Program for World-Leading Innovative R&D on Science and Technology (FIRST program); the Ministry of Education, Culture, Sports, Science, and Technology in Japan (MEXT) through the Center for NanoBio Integration (CNBI) and Grants-in-Aid for Scientific Research from MEXT (23700555 to T.S. and 24240069 to U.C.); the Japan Science and Technology Agency (JST) through the S-innovation program and COI STREAM.

References

1. P. J. Flory, *Principles of Polymer Chemistry*, Cornell University Press, ITHACA and LONDON, 1953.
2. M. Rubinstein and R. H. Colby, *Polymer Physics*, Oxford University Press, New York, 2003.
3. H. M. James and E. Guth, *J Chem Phys*, 1943, **11**, 455-481.
4. M. Shibayama, *Macromol Chem Physic*, 1998, **199**, 1-30.
5. T. Sakai, T. Matsunaga, Y. Yamamoto, C. Ito, R. Yoshida, S. Suzuki, N. Sasaki, M. Shibayama and U. I. Chung, *Macromolecules*, 2008, **41**, 5379-5384.
6. T. Sakai, *React Funct Polym*, 2013, **73**, 898-903.
7. K. Nishi, K. Fujii, M. Chijiishi, Y. Katsumoto, U. Chung, T. Sakai and M. Shibayama, *Macromolecules*, 2012, **45**, 1031-1036.
8. T. Matsunaga, T. Sakai, Y. Akagi, U. Chung and M. Shibayama, *Macromolecules*, 2009, **42**, 1344-1351.
9. T. Matsunaga, T. Sakai, Y. Akagi, U. I. Chung and M. Shibayama, *Macromolecules*, 2009, **42**, 6245-6252.
10. F. Lange, K. Schwenke, M. Kurakazu, Y. Akagi, U. I. Chung, M. Lane, J. U. Sommer, T. Sakai and K. Saalwachter, *Macromolecules*, 2011, **44**, 9666-9674.
11. Y. Akagi, J. P. Gong, U. Chung and T. Sakai, *Macromolecules*, 2013, **46**, 1035-1040.
12. P. J. Flory, *J Chem Phys*, 1977, **66**, 5720-5729.
13. G. J. Lake and A. G. Thomas, *Proc R Soc Lon Ser-A*, 1967, **300**, 108-&.
14. A. N. Gent and R. H. Tobias, *J Polym Sci Pol Phys*, 1982, **20**, 2051-2058.
15. A. N. Gent, *Langmuir*, 1996, **12**, 4492-4496.
16. P. G. deGennes, *Langmuir*, 1996, **12**, 4497-4500.
17. K. Okumura, *Europhys Lett*, 2004, **67**, 470-476.
18. Y. Tanaka, R. Kuwabara, Y. H. Na, T. Kurokawa, J. P. Gong and Y. Osada, *J Phys Chem B*, 2005, **109**, 11559-11562.
19. M. Huang, H. Furukawa, Y. Tanaka, T. Nakajima, Y. Osada and J. P. Gong, *Macromolecules*, 2007, **40**, 6658-6664.
20. S. M. Liang, Z. L. Wu, J. Hu, T. Kurokawa, Q. M. Yu and J. P. Gong, *Macromolecules*, 2011, **44**, 3016-3020.
21. Y. Akagi, H. Sakurai, J. P. Gong, U. Chung and T. Sakai, *J Chem Phys*, 2013, **139**.

22. S. Kondo, U. Chung and T. Sakai, *Polym J*, 2014, **46**, 14-20.
23. S. Kondo, H. Sakurai, U. I. Chung and T. Sakai, *Macromolecules*, 2013, **46**, 7027-7033.
24. D. R. Miller and C. W. Macosko, *Macromolecules*, 1976, **9**, 206-211.
25. Y. Akagi, T. Matsunaga, M. Shibayama, U. Chung and T. Sakai, *Macromolecules*, 2010, **43**, 488-493.
26. K. Nishi, M. Chijiishi, Y. Katsumoto, T. Nakao, K. Fujii, U. Chung, H. Noguchi, T. Sakai and M. Shibayama, *J Chem Phys*, 2012, **137**, 224903.
27. F. Oesterhelt, M. Rief and H. E. Gaub, *New J Phys*, 1999, **1**.
28. Ferry Kienberger, Vassili Ph. Pastushenko, Gerald Kada, Hermann J. Gruber, Christian Riener, H. Schindler and P. Hinterdorfer, *Single Molecules*, 2000, **1**, 123-128.
29. S. Zou, H. Schonherr and G. J. Vancso, *Angew Chem Int Edit*, 2005, **44**, 956-959.
30. Y. Tanaka, *Euro Physics Letter*, 2007, **78**, 56005.
31. H. R. Brown, *Macromolecules*, 2007, **40**, 3815-3818.
32. T. Nakajima, Y. Fukuda, T. Kurokawa, T. Sakai, U. Chung, J. P. Gong, *ACS Macro Letters*, 2013, **2**, 518-521.